

# Kinetics and Yields of Pesticide Biodegradation at Low Substrate Concentrations and under Conditions Restricting Assimilable Organic Carbon

Damian E. Helbling,<sup>a,b</sup> Frederik Hammes,<sup>a</sup> Thomas Egli,<sup>a,c</sup> Hans-Peter E. Kohler<sup>a</sup>

Eawag, Swiss Federal Institute of Aquatic Science and Technology, Department of Environmental Microbiology, Dübendorf, Switzerland<sup>a</sup>; School of Civil and Environmental Engineering, Cornell University, Ithaca, New York, USA<sup>b</sup>; Microbes-in-Water GmbH, Feldmeilen, Switzerland<sup>c</sup>

**The fundamentals of growth-linked biodegradation occurring at low substrate concentrations are poorly understood. Substrate utilization kinetics and microbial growth yields are two critically important process parameters that can be influenced by low substrate concentrations. Standard biodegradation tests aimed at measuring these parameters generally ignore the ubiquitous occurrence of assimilable organic carbon (AOC) in experimental systems which can be present at concentrations exceeding the concentration of the target substrate. The occurrence of AOC effectively makes biodegradation assays conducted at low substrate concentrations mixed-substrate assays, which can have profound effects on observed substrate utilization kinetics and microbial growth yields. In this work, we introduce a novel methodology for investigating biodegradation at low concentrations by restricting AOC in our experiments. We modified an existing method designed to measure trace concentrations of AOC in water samples and applied it to systems in which pure bacterial strains were growing on pesticide substrates between 0.01 and 50 mg liter<sup>-1</sup>. We simultaneously measured substrate concentrations by means of high-performance liquid chromatography with UV detection (HPLC-UV) or mass spectrometry (MS) and cell densities by means of flow cytometry. Our data demonstrate that substrate utilization kinetic parameters estimated from high-concentration experiments can be used to predict substrate utilization at low concentrations under AOC-restricted conditions. Further, restricting AOC in our experiments enabled accurate and direct measurement of microbial growth yields at environmentally relevant concentrations for the first time. These are critical measurements for evaluating the degradation potential of natural or engineered remediation systems. Our work provides novel insights into the kinetics of biodegradation processes and growth yields at low substrate concentrations.**

The global use of pesticides to increase crop yields and control unwanted organisms has resulted in extensive pollution to water resources. This pollution can impair water quality (1, 2) and lead to significant economic effects when pollutant concentrations warrant closure or mandated remediation of a contaminated drinking water source (3, 4). Exploitation of microbial processes has long been considered an attractive option to remediate contaminated water resources (5). However, there are unique challenges inherent in developing remediation strategies for pesticide-contaminated waters. One major challenge is the occurrence of most pesticides at low (sub-microgram/liter) concentrations (6); the fundamentals of growth-linked biodegradation occurring at these low concentrations remain poorly understood.

Substrate utilization kinetics and microbial growth yields are two critically important biodegradation process parameters. Previous research has reported that substrate utilization kinetics can differ significantly at substrate concentrations below a certain threshold (on the order of 100  $\mu\text{g liter}^{-1}$ ) compared to high concentrations (7–10), a phenomenon attributed to the presence of at least two separate, concentration-dependent uptake and transformation systems (7, 10). The consequence of these multiphasic kinetics is that extrapolation of kinetic data measured at higher concentrations may significantly under- or overestimate observed kinetics at low, environmentally relevant concentrations (10, 11). Comparatively few studies have investigated microbial growth and yield of bacterial strains at low substrate concentrations (12, 13). Several authors have reported threshold concentrations (typically less than 10  $\mu\text{g liter}^{-1}$ ) below which degradation continues in a nongrowth regime (9, 11, 14), but these conclusions are based

solely on observed first-order substrate utilization kinetics; direct measurements of microbial growth or yield at these low concentrations have not been reported.

A major limitation in interpreting previous studies on biodegradation at low concentrations is the ubiquitous presence of contaminating assimilable organic carbon (AOC) in experimental systems. Even with extreme preparative measures, it is not possible to limit AOC concentrations in experimental systems to below 5 to 10  $\mu\text{g liter}^{-1}$  (15). Experience in our lab suggests that experiments conducted with mineral medium in glassware treated according to standard laboratory practices can contain up to 100-fold more AOC than experiments conducted with more rigorously treated glassware (15). In fact, it can be assumed that growth experiments that were conducted in glassware and mineral medium prepared according to standard laboratory procedures may have contained up to 1 mg liter<sup>-1</sup> of contaminating AOC as the extent of growth in negative controls could not be distinguished from growth in experiments conducted with up to 1 mg liter<sup>-1</sup> of substrate (12, 16,

Received 5 November 2013 Accepted 2 December 2013

Published ahead of print 6 December 2013

Address correspondence to Damian E. Helbling, damian.helbling@cornell.edu.

Supplemental material for this article may be found at <http://dx.doi.org/10.1128/AEM.03622-13>.

Copyright © 2014, American Society for Microbiology. All Rights Reserved.  
doi:10.1128/AEM.03622-13

17). In effect, this implies that any biodegradation assay conducted at low substrate concentrations (below approximately 1 mg liter<sup>-1</sup>) is a mixed-substrate assay, which will inevitably have profound effects on both substrate utilization kinetics (18–20) and yield measurements (12, 21). Therefore, experiments designed to quantify substrate utilization kinetics and microbial growth yields at low substrate concentrations should include appropriate measures to minimize the interfering effects of contaminating AOC.

The goal of this work was to measure substrate utilization kinetics and microbial growth yields of pesticide biodegradation under AOC-restricted conditions. With respect to substrate utilization kinetics, we hypothesized that previously reported multiphasic kinetics can also be explained as the result of a shift from single-substrate utilization to mixed-substrate utilization. Therefore, we surmised that minimizing the concentration of interfering AOC in our experimental system would help to resolve these kinetic issues. With respect to microbial growth yields, we expect that restricting the AOC in our experiments will allow us to accurately and directly measure yield at environmentally relevant concentrations for the first time. To meet this goal, we modified an existing method designed to measure trace concentrations of AOC in water samples and applied it to systems where pure bacterial strains were growing on pesticide substrates at concentrations between 0.01 and 50 mg liter<sup>-1</sup>. We simultaneously measured substrate concentrations by means of high-performance liquid chromatography with UV detection (HPLC-UV) or mass spectrometry (MS) and cell densities by means of flow cytometry. We used data derived from high-concentration experiments to estimate substrate utilization kinetic parameters. The parameters were used to simulate substrate utilization at lower concentrations and were compared directly to measured data. Microbial growth yields were likewise calculated over a range of concentrations. Here, we present a novel methodology for investigating biodegradation at low concentrations, and the results provide novel insights into the kinetics of biodegradation processes and growth yields at low substrate concentrations.

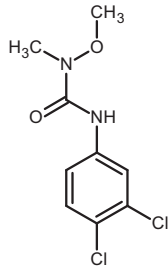
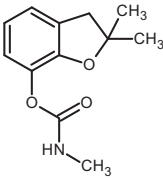
## MATERIALS AND METHODS

**Chemicals.** All chemicals were reagent grade. Linuron (99.5% purity) was purchased from Ehrenstorfer GmbH (Augsburg, Germany). Carbofuran (99.9% purity) was purchased from Sigma-Aldrich (Seelze, Germany). Spike solutions were maintained in AOC-restricted mineral medium at concentrations of 50 mg liter<sup>-1</sup> for linuron and 100 mg liter<sup>-1</sup> for carbofuran. Chemical structures along with relevant physicochemical and thermodynamic properties are provided in Table 1.

**Strains.** The bacterial strains investigated included the linuron degrader *Variovorax* sp. strain SRS16 and the carbofuran degrader *Novosphingobium* sp. strain KN65.2. These strains were selected as candidates for engineered biological processes targeting two specific pesticide pollutants typically found at trace concentrations in groundwater, a primarily AOC-restricted habitat (22). *Variovorax* sp. SRS16 was received as a streak on R2A agar plates from S. Sørensen (Department of Geochemistry, Geological Survey of Denmark and Greenland). *Novosphingobium* sp. KN65.2 was received as a streak on an R2A agar plate from D. Springael (Department of Earth and Environmental Sciences, Katholieke Universiteit [KU] Leuven). For each strain, a single colony was picked from the agar plate and added to 5 ml of sterilized LB medium. Cells were grown to early stationary phase and diluted to approximately 15% glycerol (0.5 ml of 50% sterile glycerol added to 1 ml of cell culture) and stored at –80°C.

**AOC-restricted mineral medium.** Experiments were conducted in a synthetic, AOC-restricted mineral medium containing 3.73 g liter<sup>-1</sup>

TABLE 1 Chemical structures and relevant physicochemical and thermodynamic properties

Characteristic	Linuron	Carbofuran
Structure		
CAS no. <sup>h</sup>	330-55-2	1563-66-2
Molecular formula	C <sub>9</sub> H <sub>10</sub> Cl <sub>2</sub> N <sub>2</sub> O <sub>2</sub>	C <sub>12</sub> H <sub>15</sub> NO <sub>3</sub>
Molecular mass (Da)	248.0113	221.1046
log K <sub>ow</sub> <sup>a</sup>	2.91	2.30
Solubility (mg liter <sup>-1</sup> ) <sup>b</sup>	44.27	353.9
Henry's constant (atm m <sup>3</sup> mol <sup>-1</sup> ) <sup>c</sup>	1.15 × 10 <sup>-08</sup>	1.63 × 10 <sup>-09</sup>
pK <sub>a</sub> <sup>d</sup>	11.9	14.8
Degree of reductance (γ <sub>D</sub> )	4.44	4.67
ΔG <sub>CS</sub> <sup>0'</sup> (kJ mol <sup>-1</sup> ) <sup>e</sup>	–276.14	–251.46
ΔG <sub>D</sub> <sup>0'</sup> (kJ e <sup>-</sup> equivalent <sup>-1</sup> ) <sup>f</sup>	34.81	29.48
Theoretical Y <sub>C/C</sub> <sup>g</sup>	0.39	0.41

<sup>a</sup> K<sub>ow</sub> is the octanol-water partition coefficient, estimated from KOWWIN, version 1.67 (46).

<sup>b</sup> Water solubility at 25°C from WSKOW, version 1.41 (46).

<sup>c</sup> Henry's constant from HENRYWIN, version 3.10 (46).

<sup>d</sup> pK<sub>a</sub> values were estimated using MarvinSketch, version 5.11.3, from ChemAxon (Cambridge, MA).

<sup>e</sup> Gibbs energy of formation of each substrate estimated according to the group contribution approach (47, 48).

<sup>f</sup> Gibbs free energy of the electron donor half-reaction for each substrate.

<sup>g</sup> Theoretical yield (Y<sub>C/C</sub>, calculated as mol of C in cells per mol of C in substrate) was estimated using the McCarty efficiency approach (32, 37–39).

<sup>h</sup> CAS, Chemical Abstract Services.

KH<sub>2</sub>PO<sub>4</sub>, 2.24 g liter<sup>-1</sup> Na<sub>2</sub>HPO<sub>4</sub> · 2H<sub>2</sub>O, 120 mg liter<sup>-1</sup> (NH<sub>4</sub>)<sub>2</sub>SO<sub>4</sub>, 70 mg liter<sup>-1</sup> MgSO<sub>4</sub>, and 1 mg liter<sup>-1</sup> Ca(NO<sub>3</sub>)<sub>2</sub> at a pH of 6.5. Trace elements were added to final concentrations of 100 μg liter<sup>-1</sup> H<sub>3</sub>BO<sub>3</sub>, 2.5 mg liter<sup>-1</sup> FeSO<sub>4</sub> · 7H<sub>2</sub>O, 750 μg liter<sup>-1</sup> MnSO<sub>4</sub> · H<sub>2</sub>O, 1.3 mg liter<sup>-1</sup> ZnSO<sub>4</sub> · 7H<sub>2</sub>O, 250 μg liter<sup>-1</sup> CuSO<sub>4</sub> · 5H<sub>2</sub>O, 300 μg liter<sup>-1</sup> Co(NO<sub>3</sub>)<sub>2</sub> · 6H<sub>2</sub>O, 150 μg liter<sup>-1</sup> Na<sub>2</sub>MoO<sub>4</sub> · 2H<sub>2</sub>O, and 10 μg liter<sup>-1</sup> NiSO<sub>4</sub> · 7H<sub>2</sub>O. The mineral medium recipe was modified from recipes previously described for cultivation of each strain on its target substrate (23; T. P. O. Nguyen, D. E. Helbling, K. Bers, T. T. Fida, R. Wattiez, H. P.-E. Kohler, R. De Mot, D. Springael, submitted for publication).

**Inoculum preparation.** A sterile loop was used to inoculate frozen cells maintained in 15% glycerol at –80°C into 5 ml of sterilized 10-fold-diluted LB growth medium amended with approximately 10 mg liter<sup>-1</sup> of the target substrate. Cells were grown at 30°C to late exponential phase, at which point 1 ml of culture was sampled, centrifuged at 5,000 × g for 5 min, carefully decanted, and resuspended in an equal volume of AOC-restricted mineral medium. This washing procedure was repeated three times. The final cell density was determined by means of flow cytometry. Cells were subsequently inoculated at 10<sup>5</sup> cells ml<sup>-1</sup> into 20 ml of mineral medium amended with approximately 10 mg liter<sup>-1</sup> of the target substrate. Cells were incubated until the chemical was completely degraded (monitored by HPLC-UV), at which point 1 ml of culture was sampled, centrifuged at 5,000 × g for 5 min, carefully decanted, and resuspended in an equal volume of AOC-restricted mineral medium. This washing procedure was again repeated three times to ensure complete removal of residual AOC. The final inoculum concentration was determined by means of flow cytometry.

**Incubation experiments.** All experiments were designed based on methods previously established for measuring bacterial growth on trace concentrations of AOC (15). Briefly, experiments were conducted in 40-ml carbon-free borosilicate glass vials. All glassware and caps were treated rigorously to remove residual AOC as previously described (15, 24, 25). Microbial growth and substrate utilization were measured in 20 ml of AOC-restricted mineral medium amended with the target substrates. A series of three incubation experiments was designed to address three main objectives. First, high-concentration incubation experiments were conducted in triplicate at approximate initial conditions of  $10^5$  cells  $\text{ml}^{-1}$  and 50  $\text{mg liter}^{-1}$  of the target substrate to confirm growth-linked substrate utilization for each strain-substrate pair. Second, low-concentration incubation experiments were conducted under a matrix of initial cell densities ( $10^6$ ,  $10^5$ ,  $10^4$ , and  $10^3$  cells  $\text{ml}^{-1}$ ) and substrate concentrations (10, 3, 1, 0.3, 0.1, 0.03, and 0.01  $\text{mg liter}^{-1}$ ) to systematically investigate the effects of stepwise changes in initial conditions on microbial growth and substrate utilization. Third, a series of incubation experiments was conducted at an initial cell density of  $10^5$  cells  $\text{ml}^{-1}$  and a range of initial substrate concentrations from 1 to 50  $\text{mg liter}^{-1}$  to obtain an optimal data set for estimation of kinetic parameters. All reaction mixtures were incubated at 30°C until cells attained stationary phase or until the measured substrate concentration was below the limit of detection. Samples were taken at the time of inoculation and periodically thereafter to measure cell growth by means of flow cytometry and substrate concentration by means of HPLC-UV or HPLC-MS. As a positive control,  $10^3$  cells  $\text{ml}^{-1}$  was inoculated into 5 ml of sterilized LB medium, and growth was confirmed by visual inspection of changes in optical density. As negative controls, incubation experiments were run in the absence of either cells or substrate.

**Flow cytometry.** Cell densities were measured on a BD Accuri C6 Flow Cytometer (Erembodegem, Belgium). Aliquots of 500  $\mu\text{l}$  from an incubation experiment were combined with 5  $\mu\text{l}$  of SYBR green stain (Molecular Probes, Basel, Switzerland) diluted 100-fold in dimethyl sulfoxide (Fluka Chemie AG, Buchs, Switzerland) in a 1.5-ml plastic centrifuge tube (Greiner Bio One, Frickenhausen, Germany), vortexed briefly, and incubated in the dark at 40°C for 10 min. For cell densities of less than  $5 \times 10^5$  cells  $\text{ml}^{-1}$ , samples were measured directly on a BD Accuri C6 Flow Cytometer without dilution. In the case of higher cell densities, samples were appropriately diluted with 0.1- $\mu\text{m}$ -pore-size-filtered bottled mineral water (Evian, France) to achieve a cell density in the range of  $3 \times 10^3$  cells  $\text{ml}^{-1}$  and  $5 \times 10^5$  cells  $\text{ml}^{-1}$ . Data were analyzed with the CFlow, version 1.0.227.4, flow cytometry software. For all strains, enumeration was achieved with signals collected on the gated combined 533 nm/670 nm density plot (26).

**Chemical analysis.** Chemical analysis was conducted on either an HPLC-UV (0.3 to 50  $\text{mg liter}^{-1}$  experiments) or HPLC-MS (0.01 to 0.3  $\text{mg liter}^{-1}$  experiments) instrument. HPLC-UV analyses were performed on a Gynkotek system with a Dionex ASI-100 autosampler and a UVD 340U diode array detector. Compounds were separated on a Nucleosil 100-5 C<sub>18</sub> HD column (250 by 4.0 mm) with an octadecyl modified high-density silica stationary phase (Macherey-Nagel, Düren, Germany). The system was operated isocratically at a flow rate of 0.7  $\text{ml min}^{-1}$  with different eluents and detection wavelengths for carbofuran (55% methanol and 45% nanopure water) and linuron (70% methanol and 30% nanopure water; 213 nm). Limits of quantification of HPLC-UV were less than 0.05  $\text{mg liter}^{-1}$  with a 50- $\mu\text{l}$  injection volume. The Chromeleon Client, version 6.6 (Dionex), was used for chromatogram analysis and interpretation. HPLC-MS analyses were performed on a high-resolution mass spectrometer (QExactive, Thermo, Waltham, MA, USA) with an analytical method that was previously described (27, 28). Briefly, compounds were separated on an XBridge (Waters, Milford, MA) C<sub>18</sub> column (2.1 mm by 50 mm; particle size, 3.5  $\mu\text{m}$ ) at a flow rate of 200  $\mu\text{l min}^{-1}$ . The mobile phase consisted of nanopure water and HPLC-grade methanol (Acros Organics, Geel, Belgium), each amended with 0.1% (volume) formic acid (98 to 100%; Acros Organics, Geel, Belgium). Samples were

injected into the column at 20  $\mu\text{l}$  with an initial mobile phase of 90:10 water/methanol, and elution from the column was achieved with a final mobile phase of 5:95 water/methanol. The QExactive spectrometer was used with electrospray ionization in positive mode. XCalibur, version 2.0.7, software (Thermo, Waltham, MA) was used for chromatogram analysis and interpretation. Limits of quantification for each compound on HPLC-MS were less than 0.001  $\text{mg liter}^{-1}$ .

**Dry weight of cells.** The dry weight of cells ( $X_{\text{DW}}$ ) was measured by first collecting stationary-phase cells on an oven-dried 0.2- $\mu\text{m}$ -pore-size Nuclepore polycarbonate track-etched membrane filter (Whatman, Piscataway, NJ, USA). The wetted filter was then dried at 105°C, and the  $X_{\text{DW}}$  given as the mass per cell was calculated as:

$$X_{\text{DW}} = \frac{(m_f - m_i)}{V \times X_s} \quad (1)$$

where  $m_f$  is the mass of the dry filter after filtration (mg),  $m_i$  is the mass of the dry filter before filtration (mg),  $V$  is the volume of stationary-phase cells filtered (ml), and  $X_s$  is the stationary-phase cell density determined by means of flow cytometry (cells  $\text{ml}^{-1}$ ).

**Estimation of kinetic parameters.** Microbial growth and substrate utilization parameters were estimated from the experimental data by assuming Monod kinetics as given in equations 2 and 3 (29):

$$\frac{dX}{dt} = \frac{\mu_{\text{max}} S}{K_s + S} X \quad (2)$$

$$\frac{dS}{dt} = \frac{1}{Y_{C/C}} \frac{\mu_{\text{max}} S}{K_s + S} X \quad (3)$$

where  $S$  is the concentration of carbon in the substrate ( $\text{mM } C_{\text{substrate}}$ ),  $\mu_{\text{max}}$  is the maximum specific growth rate ( $\text{day}^{-1}$ ),  $K_s$  is the concentration of carbon in the substrate giving one-half the maximum rate ( $\text{mM } C_{\text{substrate}}$ ),  $X$  is the biomass concentration of carbon in cells ( $\text{mM } C_{\text{cells}}$ ), and  $Y_{C/C}$  is the molar yield in mol of carbon in cells per mol of carbon in the substrate ( $\text{mol of } C_{\text{cells}} \times \text{mol of } C_{\text{substrate}}^{-1}$ ). All concentrations were converted to millimolar carbon for consistency and to follow the previously established convention (30–32). Cell densities measured by means of flow cytometry in units of cells  $\text{ml}^{-1}$  were converted to  $\text{mM } C_{\text{cells}}$  by using the measured dry weight of cells ( $X_{\text{DW}}$ ) and an assumed molecular weight of cells of 22.6  $\text{g } X_{\text{DW}} \text{ C mol}^{-1}$  (32) and by assuming that the organic cell formulation  $\text{CH}_{1.4}\text{O}_{0.4}\text{N}_{0.2}$  is 95% of the  $X_{\text{DW}}$  (33).

We used R, version 3.0.0 (34), and the flexible modeling environment (FME) package (35) to numerically and simultaneously solve the differential equations provided in equations 2 and 3 and to estimate the values of  $\mu_{\text{max}}$ ,  $K_s$ , and  $Y_{C/C}$  by minimizing the sum of the squared residuals between measured and modeled data. We then used a Markov chain Monte Carlo (MCMC) method that uses a delayed rejection and adaptive Metropolis procedure (36) to construct a Markov chain and sample from probability distributions over 50,000 iterations to generate a marginal distribution of parameter values to assess uncertainty and drift in the parameter estimates.

**Estimation of theoretical and experimental molar yield.** The theoretical molar yield for each substrate was estimated by using the efficiency approach of McCarty (32, 37–39). We further adjusted theoretical molar yield predictions to account for putative oxygenase activation reactions through a previously described method (33). More information on the procedures to estimate theoretical molar yield along with an example calculation for carbofuran is provided in the supplemental material.

Experimental yield is reported as numeric yield (i.e.,  $Y_{\#}$ , yield reported as cell numbers per mass of substrate) and as molar yield (i.e.,  $Y_{C/C}$ , yield reported as moles of cell carbon per moles of substrate carbon). Numeric yield was estimated as:

$$Y_{\#} = \frac{(S_0 - S_s)}{(X_s - X_{sc})} \quad (4)$$

where  $Y_{\#}$  is the numeric yield (cells  $\mu\text{g substrate}^{-1}$ ),  $S_0$  is the initial substrate concentration ( $\mu\text{g ml}^{-1}$ ),  $S_s$  is the residual substrate concentra-



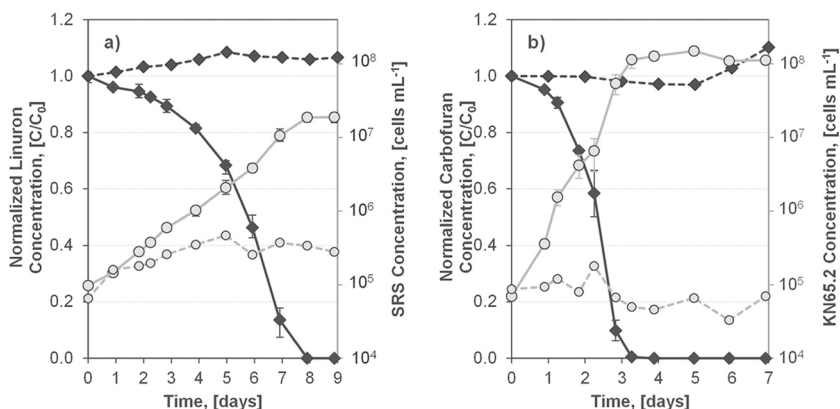


**FIG 1** Growth and substrate utilization in high-concentration incubation experiments for *Variovorax* sp. SRS16 with linuron ( $X_0 = 9.8 \times 10^4 \pm 8 \times 10^3$  cells  $\text{ml}^{-1}$ ;  $S_0 = 33.6 \pm 0.7$  mg  $\text{liter}^{-1}$ ) (a) and *Novosphingobium* sp. KN65.2 with carbofuran ( $X_0 = 7.0 \times 10^4 \pm 6 \times 10^3$  cells  $\text{ml}^{-1}$ ;  $S_0 = 45.1 \pm 0.5$  mg  $\text{liter}^{-1}$ ) (b). Solid lines represent the average of three replicate experiments for cell growth (gray circles) and substrate utilization (black diamonds). The dashed lines are the negative controls for no cells (black diamonds) and no substrate (gray circles).  $X_0$  is the initial cell density.  $S_0$  is the initial substrate concentrations.

tion remaining when cells reach stationary phase ( $\mu\text{g ml}^{-1}$ ),  $X_s$  is the cell density at stationary phase (cells  $\text{ml}^{-1}$ ), and  $X_{s,c}$  is the cell density at stationary phase in the no-substrate negative control (cells  $\text{ml}^{-1}$ ). Numeric yield was converted to molar yield by using the dry weight of cells ( $X_{\text{DW}}$ ) and an assumed molecular weight of cells of  $22.6 \text{ g } X_{\text{DW}} \text{ C mol}^{-1}$  (32) and by assuming that the organic cell formulation  $\text{CH}_{1.4}\text{O}_{0.4}\text{N}_{0.2}$  is 95% of the  $X_{\text{DW}}$  (33).

## RESULTS AND DISCUSSION

**AOC concentrations in mineral medium.** The goal of this work was to measure substrate utilization kinetics and microbial growth yields at low substrate concentrations and under AOC-restricted conditions. We therefore first sought to determine the concentration of background AOC in our experimental system. To do this, we inoculated each strain into the mineral medium at initial cell densities of  $10^3$  cells  $\text{ml}^{-1}$ . Cell densities measured after 7 days were  $1.3 \times 10^5$  and  $6.6 \times 10^4$  cells  $\text{ml}^{-1}$ , which corresponds to the nutritional equivalent of 13 and  $6.6 \mu\text{g liter}^{-1}$  of AOC for strains SRS16 and KN65.2, respectively, using standard yield conversion factors (15). Achieving these low concentrations of background AOC enabled quantification of substrate utilization kinetics and microbial growth yield on target substrates down to approximately  $10 \mu\text{g liter}^{-1}$ ; experiments conducted below this limit would be difficult to interpret due to the influence of background AOC.

**High-concentration incubation experiments.** The first set of incubation experiments were designed to confirm growth-linked substrate utilization for both strain-substrate pairs under AOC-restricted conditions; both of the strains selected for this work have previously been shown to mineralize a target pesticide over a wide range of concentrations (40; Nguyen et al., submitted), but so far only limited data on growth and yield have been reported (see the supplemental material for the discussion on each strain). The results of these experiments are presented in Fig. 1. High-concentration incubation experiments were conducted at initial conditions of approximately  $50 \text{ mg liter}^{-1}$  of substrate and  $10^5$  cells  $\text{ml}^{-1}$ . Under these conditions, strains SRS16 and KN65.2 grew as shown in Fig. 1a and b, respectively. Stationary phase was attained within 9 days, and cell densities exceeded  $10^7$  cells  $\text{ml}^{-1}$  in experiments with strain SRS16; stationary phase was attained within 4 days, and cell densities exceeded  $10^8$  cells  $\text{ml}^{-1}$  in exper-

iments with strain KN65.2. No residual linuron or carbofuran concentrations were measured. In negative controls, there was no measurable growth in the AOC-restricted mineral medium in the absence of the pesticide substrate (growth on the background AOC was less than the initial cell density of these experiments) and pesticides did not disappear in the absence of cells (Fig. 1, dashed lines).

**Low-concentration incubation experiments.** In the second set of incubation experiments, we aimed to measure substrate utilization and microbial growth over a range of initial substrate concentrations and cell densities to elucidate the effects of step-wise changes in initial conditions on substrate utilization kinetics and microbial growth yields. We designed a matrix of 28 incubation experiments investigating seven initial substrate concentrations and four initial cell densities. We selected initial substrate concentrations between  $0.01$  and  $10 \text{ mg liter}^{-1}$  to test for shifts in substrate utilization kinetics below previously reported thresholds for multiphasic kinetics on the order of  $100 \mu\text{g liter}^{-1}$  (7–10). We selected initial cell densities between  $10^3$  to  $10^6$  cells  $\text{ml}^{-1}$  to likewise test for shifts in substrate utilization kinetics in potential growth (high ratio of substrate concentration to cell density) and nongrowth (low ratio of substrate concentration to cell density) regimes (9, 11, 14). A summary of substrate utilization observed in these incubation experiments is provided in Fig. 2, where the fraction of the initial substrate concentration remaining after incubation periods of 3 and 28 days is reported.

The effect of lowering initial substrate concentrations and cell densities on the extent and kinetics of substrate utilization varied considerably between the two strains. In experiments with strain SRS16, the extent of substrate utilization was unaffected by lower initial substrate concentrations and cell densities; we observed partial substrate utilization in all incubations after an incubation period of 3 days (Fig. 2a) and nearly complete substrate utilization after an incubation period of 28 days (Fig. 2b). In experiments with strain KN65.2, substrate utilization was apparently affected by both lower initial substrate concentrations and cell densities. We observed nearly no substrate utilization after an incubation period of 3 days (Fig. 2c) and a bipartite substrate utilization pattern after an incubation period of 28 days (Fig. 2d); complete substrate utilization was observed for most incubations with the

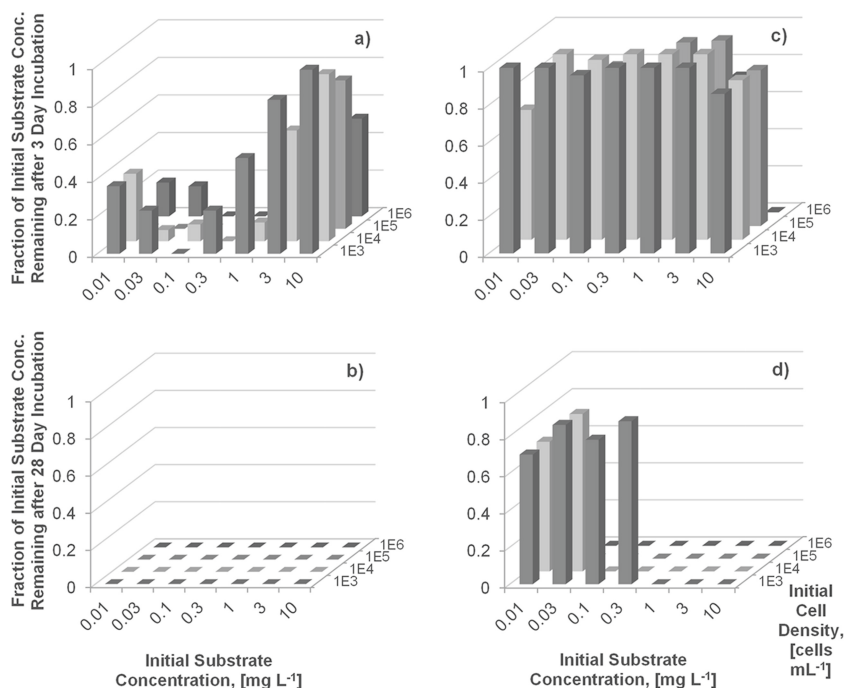


FIG 2 The fraction of initial substrate concentration remaining after incubation periods of 3 and 28 days for *Variovorax* sp. SRS16 with linuron (a and b) and *Novosphingobium* sp. KN65.2 with carbofuran (c and d).

exception of those at initial cell densities of  $10^3$  and  $10^4$  cells  $\text{mL}^{-1}$  and initial substrate concentrations below  $1 \text{ mg liter}^{-1}$  and  $0.1 \text{ mg liter}^{-1}$ , respectively, where we observed nearly no substrate utilization.

**Incubation experiments for kinetic parameter estimation.** Estimating parameters to describe Monod growth and substrate utilization kinetics from experimental data is problematic due to the potential colinearity of  $\mu_{\max}$  and  $K_s$  (41). Other investigators have demonstrated that optimal experimental conditions can be established to limit the colinearity of  $\mu_{\max}$  and  $K_s$ , thus rendering those parameters identifiable (42, 43). Optimal conditions are based on ratios between the initial cell and substrate concentrations and the magnitude of  $\mu_{\max}$  and  $K_s$ . Because we had no *a priori* knowledge of the magnitude of  $\mu_{\max}$  and  $K_s$ , we designed a series of independent incubation experiments to obtain an optimal data set for estimation of kinetic parameters. These experiments were conducted at an initial cell density of  $10^5$  cells  $\text{mL}^{-1}$  and at initial substrate concentrations between  $1$  and  $50 \text{ mg liter}^{-1}$  to obtain substrate utilization and microbial growth data encompassing a wide range of ratios between initial cell densities and substrate concentrations. We then selected the experimental conditions that produced the lowest colinearity between  $\mu_{\max}$  and  $K_s$  and highest identifiability of all parameters based on an analysis of Markov chain traces and pairs plots. The optimal data set for kinetic parameter estimation was identified at an initial cell density of  $10^5$  cells  $\text{mL}^{-1}$  and initial substrate concentrations of  $1 \text{ mg liter}^{-1}$  and  $10 \text{ mg liter}^{-1}$  in experiments with strains SRS16 and KN65.2, respectively (see supplemental material for details). The model fits to the experimental data for the optimal data sets are provided in Fig. 3. The estimated parameter values and standard deviations of the marginal distributions are provided in Table 2.

Noteworthy are the magnitude of the estimates for  $\mu_{\max}$  and  $K_s$

for each strain. The  $\mu_{\max}$  estimate for strain SRS16 ( $1.3 \text{ day}^{-1}$ ) is six times lower than the estimate for strain KN65.2 ( $7.8 \text{ day}^{-1}$ ). However, the  $K_s$  estimate for strain SRS16 ( $0.0029 \text{ mM C}$  or  $0.06 \text{ mg liter}^{-1}$ ) is 2 orders of magnitude lower than the estimate for strain KN65.2 ( $0.54 \text{ mM C}$  or  $10 \text{ mg liter}^{-1}$ ). Taken together, these parameters suggest that while strain KN65.2 should utilize carbofuran more rapidly than strain SRS16 utilizes linuron at high concentrations, strain SRS16 should utilize linuron more rapidly than strain KN65.2 utilizes carbofuran at low concentrations. These insights are derived from the kinetic parameters estimated from a single set of high-concentration experiments.

**Simulations of substrate utilization at low concentrations.** We hypothesized that previously reported multiphasic kinetics can be the result of a shift from single-substrate utilization to

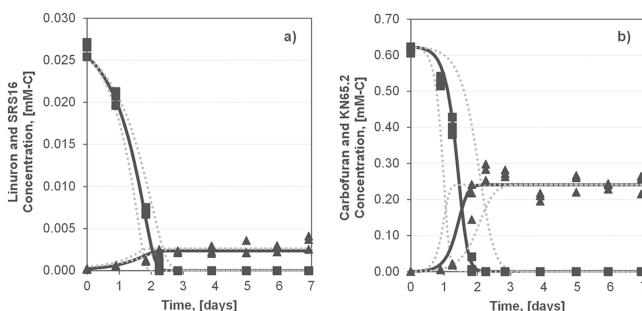


FIG 3 Comparison of simulated data (solid black lines) with 90% confidence intervals (dotted gray lines) to measured substrate utilization (squares) and microbial growth (triangles) for *Variovorax* sp. SRS16 with linuron (a) and *Novosphingobium* sp. KN65.2 with carbofuran (b). Measured data are from optimal data sets utilized for estimation of kinetic parameters used in all simulations.

TABLE 2 Estimated and measured parameters for each strain

Parameter name <sup>a</sup>	Value for the strain (substrate)	
	SRS16 (linuron)	KN65.2 (carbofuran)
Estimated kinetic parameters		
$\mu_{\max}$ (day <sup>-1</sup> )	1.3 ± 0.1	7.8 ± 1.4
$K_s$ (mM C)	0.0029 ± 0.001	0.54 ± 0.2
$Y_{C/C}$ (mol of $C_{\text{cells}}$ mol $C_{\text{substrate}}$ <sup>-1</sup> )	0.08 ± 0.01	0.39 ± 0.01
$X_{\text{DW}}$ by substrate concentration		
$S_0 = 50$ mg liter <sup>-1</sup> ( $10^{-13}$ g cell <sup>-1</sup> )	1.4	2.2
$S_0 = 10$ mg liter <sup>-1</sup> ( $10^{-13}$ g cell <sup>-1</sup> )	1.0	1.6
$S_0 = 1$ mg liter <sup>-1</sup> ( $10^{-13}$ g cell <sup>-1</sup> )	0.6	1.3
$Y_{C/C}$ (mol of $C_{\text{cells}}$ mol $C_{\text{substrate}}$ <sup>-1</sup> )		
Theoretical	0.39	0.41
Measured	0.06 ± 0.01	0.42 ± 0.07

<sup>a</sup>  $\mu_{\max}$ , the maximum specific growth rate;  $K_s$ , the half-saturation constant;  $Y_{C/C}$ , yield;  $X_{\text{DW}}$ , dry weight of cells.

mixed-substrate utilization. Therefore, we expected that restricting AOC in our experimental system would eliminate observed shifts in kinetics and enable extrapolation of kinetic parameters from high-concentration to low-concentration conditions. To test this hypothesis, we used the kinetic parameters reported in Table 2 to simulate substrate utilization under the matrix of initial conditions investigated in the low-concentration incubation experiments. We then compared the measured and simulated data for each set of initial conditions; fits of the raw data are presented in Fig. S4 and S5 of the supplemental material. A plot of the sum of the squared error (SSE) of the residuals measured between measured and simulated data are provided in Fig. 4 as a measure of the goodness of fit. All data are presented in Fig. S4 and S5 as the fraction of substrate remaining as a function of time so that the magnitude of the SSE can be compared across all experiments, regardless of initial substrate concentration.

Examination of Fig. S4 and S5 in the supplemental material and of Fig. 4 reveals that the substrate utilization kinetics measured at high concentrations predict substrate utilization at lower initial conditions well. In experiments with strain SRS16, rapid linuron utilization resulted in a limited number of nonzero data points to compare with the simulated data (see Fig. S5). Nevertheless, nearly all of the measured data (92%) fall within the 90%

confidence interval of the simulation, resulting in very low SSE values for the full matrix of initial conditions (Fig. 4a). In experiments with strain KN65.2, the bipartite behavior of observed substrate utilization shown in Fig. 2d was likewise predicted from the estimated substrate utilization kinetics; very slow utilization of carbofuran is predicted at cell inoculum concentrations of  $10^3$  and  $10^4$  cells ml<sup>-1</sup> and initial substrate concentrations below 1 mg liter<sup>-1</sup> and 0.1 mg liter<sup>-1</sup>, respectively. This confirms that the bipartite behavior is solely a consequence of substrate utilization kinetics and can be predicted with parameters estimated from high-concentration experiments. In a few cases, measured carbofuran utilization was more rapid than predicted, resulting in rather high SSE values and indicating a relatively poor performance of the model under these few sets of initial conditions. In these cases, the poor performance of the model was at the boundary of the observed bipartite behavior (Fig. 4b). Because the model accurately predicts the observed bipartite behavior of substrate utilization, we attribute these errors at the boundary to uncertainty in the estimated parameters, the magnitude of which determines the predicted boundary of the bipartite behavior. Overall, 77% of the measured data falls within the 90% confidence interval of the simulation for strain KN65.2 utilizing carbofuran.

Our results demonstrate that parameters of substrate utilization kinetics estimated at high concentrations can accurately predict substrate utilization at lower concentrations under AOC-restricted conditions. Multiphasic kinetics were not observed. While our data cannot disprove the existence of multiple, concentration-dependent uptake and transformation systems in bacteria that lead to observed shifts in substrate kinetics at low concentrations, our data are consistent with our hypothesis that observed shifts in kinetics could be the result of shifts from single-substrate utilization to mixed-substrate utilization. Published data suggest that shifts to mixed-substrate utilization can likewise result in shifts in kinetics (18–20, 44).

**Estimation of theoretical and experimental molar yield.** We also expected that restricting AOC in our experiments will enable accurate and direct measurement of yield at environmentally relevant concentrations for the first time. We estimated numeric yields from the high- and low-concentration incubation experiments (when final cell densities were significantly greater than initial cell densities) according to equation 4. Restricting the AOC in our experimental system enabled yield estimates for strains SRS16 and KN65.2 at initial substrate concentrations as low as 0.1 and 0.03 mg

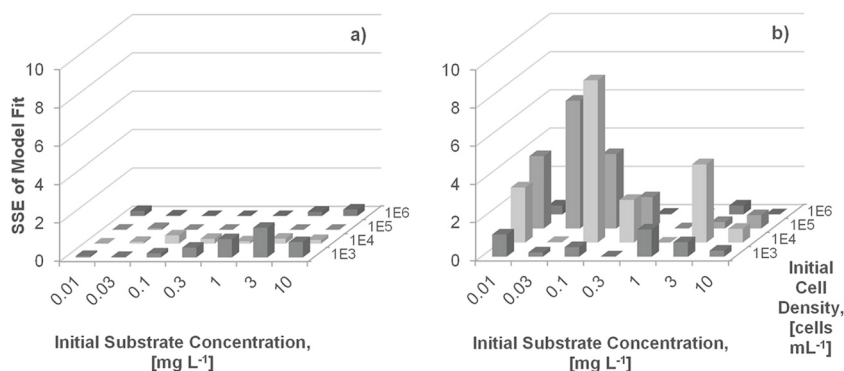


FIG 4 Sum of the squared error (SSE) for the fits of the kinetics model to the low-concentration incubation experiment data for *Variovorax* sp. SRS16 with linuron (a) and *Novosphingobium* sp. KN65.2 with carbofuran (b).

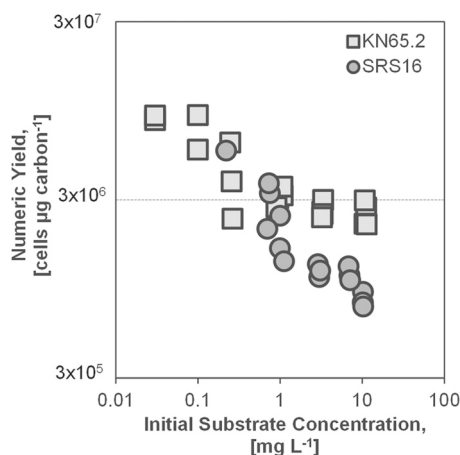


FIG 5 Numeric yield as a function of initial substrate concentration for strains KN65.2 and SRS16.

liter<sup>-1</sup>, respectively. Numeric yield over the full range of initial substrate concentrations is provided in Fig. 5. Numeric yield increased by approximately 1 order of magnitude with decreasing initial substrate concentrations for both strains. This increase in numeric yield, however, could be explained by a corresponding decrease in stationary-phase cell size ( $X_{DW}$ ) with decreasing initial substrate concentrations; it has previously been demonstrated that cellular composition and cell size are directly related to growth rate and initial substrate concentration (45). We confirmed the changes in cellular composition and cell size by measuring the  $X_{DW}$  of stationary-phase cells for strains SRS16 and KN65.2 following growth in 50 mg liter<sup>-1</sup>, 10 mg liter<sup>-1</sup>, and 1 mg liter<sup>-1</sup> of their respective pesticide substrates. Measured values of  $X_{DW}$  as a function of initial substrate concentration are reported in Table 2. Using these measured values of  $X_{DW}$ , molar yield was calculated as described in Materials and Methods. Molar yield over this range of substrate concentrations was found to be relatively constant and is reported in Table 2 as the average molar yield  $\pm$  standard deviation.

We also estimated the maximum theoretical molar yield of each substrate by using the efficiency approach of McCarty (5, 32, 38, 39). In this approach, it is assumed that yield is primarily dependent on the degree of reductance of the carbon source substrate, the Gibbs energy of formation of the carbon source substrate, and the Gibbs free energy of the electron donor half-reaction. These parameters were estimated for each substrate and are provided in Table 1 along with the theoretical molar yield. The theoretical molar yield of growth on carbofuran matches the measured molar yield for strain KN65.2. However, the theoretical molar yield of growth on linuron predicts significantly more growth than was measured for strain SRS16. There are two likely explanations for this discrepancy. One is the formation of recalcitrant metabolites that limit the amount of carbon and energy available for biomass formation though no recalcitrant metabolites were detected in acquired UV and MS chromatograms. The other is an overestimation of the theoretical molar yield due to incorrect assumptions for the magnitude of specific parameters (e.g., the efficiency constant) in the thermodynamic efficiency approach (31). More detailed analysis of the metabolite spectrum, biodegradation pathway, or biomass composition would be required to resolve this discrepancy. Nevertheless, our data show that strains SRS16 and KN65.2 degrade their target pesticide substrates by means of growth-

linked processes even at low concentrations. The molar yields are constant over large ranges of initial substrate concentrations; there were no observed shifts to a nongrowth degradation regime.

**Environmental relevance.** It is clearly important to investigate growth-linked biodegradation of trace pollutants at low, environmentally relevant concentrations. Substrate utilization kinetics and microbial growth yields are parameters of particular importance if one wishes to model pollutant removal through natural or engineered remediation systems. However, previously reported estimates of these parameters have limited utility because they are generally estimated in experimental systems that have not considered the presence of contaminating AOC, which can have profound effects on observed substrate utilization kinetics and growth yields. The novel methodology presented in this work makes estimates of these parameters under AOC-restricted conditions for the first time. The parameters estimated herein and presented in Table 2 can be used to predict substrate utilization and strain growth under a variety of scenarios.

We acknowledge that working under AOC-restricted conditions is a simplification of reality with respect to environmental systems. However, this simplification was required to isolate the specific metabolic processes we aimed to measure and to improve our fundamental understanding of biodegradation processes at low concentrations. Further, true models for the prediction of substrate utilization under environmental conditions (i.e., low substrate concentrations and in the presence of AOC and competing microbial flora) should incorporate separate measures of substrate utilization kinetics on the target substrate (as presented here) and on environmental AOC at environmentally relevant concentrations. Future work will focus on elucidating these effects of mixed-substrate availability and competing microbial flora on target pesticide utilization, strain growth, and cellular yield.

## ACKNOWLEDGMENTS

This work was funded by the EU-FP7 project titled Biotreat.

We thank S. Sørensen (Department of Geochemistry, Geological Survey of Denmark and Greenland) and D. Springael (Department of Earth and Environmental Sciences, KU Leuven, The Netherlands) for providing us with three of the strains. We thank David R. Johnson for critical discussions and for critically reading preliminary versions of the manuscript.

## REFERENCES

- Benner J, Helbling DE, Kohler HPE, Wittebol J, Kaiser E, Prasse C, Ternes TA, Albers CN, Aamand J, Horemans B, Springael D, Walravens E, Boon N. 2013. Is biological treatment a viable alternative for micropollutant removal in drinking water treatment processes? *Water Res.* 47: 5955–5976. <http://dx.doi.org/10.1016/j.watres.2013.07.015>.
- Fenner K, Canonica S, Wackett LP, Elsner M. 2013. Evaluating pesticide degradation in the environment: blind spots and emerging opportunities. *Science* 341:752–758. <http://dx.doi.org/10.1126/science.1236281>.
- Simonsen A, Badawi N, Anskjær GG, Albers CN, Sørensen SR, Sørensen J, Aamand J. 2012. Intermediate accumulation of metabolites results in a bottleneck for mineralisation of the herbicide metabolite 2,6-dichlorobenzamide (BAM) by *Aminobacter* spp. *Appl. Microbiol. Biotechnol.* 94:237–245. <http://dx.doi.org/10.1007/s00253-011-3591-x>.
- Simonsen A, Holtze MS, Sørensen SR, Sørensen SJ, Aamand J. 2006. Mineralisation of 2,6-dichlorobenzamide (BAM) in dichlobenil-exposed soils and isolation of a BAM-mineralising *Aminobacter* sp. *Environ. Pollut.* 144:289–295. <http://dx.doi.org/10.1016/j.envpol.2005.11.047>.
- Alexander M. 1981. Biodegradation of chemicals of environmental concern. *Science* 211:132–138. <http://dx.doi.org/10.1126/science.7444456>.
- Kolpin DW, Barbash JE, Gilliom RJ. 1998. Occurrence of pesticides in shallow groundwater of the United States: initial results from the national water-quality assessment program. *Environ. Sci. Technol.* 32:558–566. <http://dx.doi.org/10.1021/es970412g>.



7. Lewis DL, Hodson RE, Freeman LF, III. 1985. Multiphasic kinetics for transformation of methyl parathion by *Flavobacterium* species. *Appl. Environ. Microbiol.* 50:553–557.
8. Rapp P. 2001. Multiphasic kinetics of transformation of 1,2,4-trichlorobenzene at nano- and micromolar concentrations by *Burkholderia* sp. strain PS14. *Appl. Environ. Microbiol.* 67:3496–3500. <http://dx.doi.org/10.1128/AEM.67.8.3496-3500.2001>.
9. Toräng L, Nyholm N, Albrechtsen HJ. 2003. Shifts in biodegradation kinetics of the herbicides MCPP and 2,4-D at low concentrations in aerobic aquifer materials. *Environ. Sci. Technol.* 37:3095–3103. <http://dx.doi.org/10.1021/es026307a>.
10. Tros ME, Schraa G, Zehnder AJB. 1996. Transformation of low concentrations of 3-chlorobenzoate by *Pseudomonas* sp. strain B13: kinetics and residual concentrations. *Appl. Environ. Microbiol.* 62:437–442.
11. Boethling RS, Alexander M. 1979. Microbial degradation of organic compounds at trace levels. *Environ. Sci. Technol.* 13:989–991. <http://dx.doi.org/10.1021/es60156a012>.
12. Tarao M, Seto M. 2000. Estimation of the yield coefficient of *Pseudomonas* sp. strain DP-4 with a low substrate (2,4-dichlorophenol [DCP]) concentration in a mineral medium from which uncharacterized organic compounds were eliminated by a non-DCP-degrading organism. *Appl. Environ. Microbiol.* 66:566–570. <http://dx.doi.org/10.1128/AEM.66.2.566-570.2000>.
13. Seto M, Alexander M. 1985. Effect of bacterial density and substrate concentration on yield coefficients. *Appl. Environ. Microbiol.* 50:1132–1136.
14. Boethling RS, Alexander M. 1979. Effect of concentration of organic chemicals on their biodegradation by natural microbial communities. *Appl. Environ. Microbiol.* 37:1211–1216.
15. Hammes FA, Egli T. 2005. New method for assimilable organic carbon determination using flow-cytometric enumeration and a natural microbial consortium as inoculum. *Environ. Sci. Technol.* 39:3289–3294. <http://dx.doi.org/10.1021/es048277c>.
16. Sørensen SR, Holtz MS, Simonsen A, Aamand J. 2007. Degradation and mineralization of nanomolar concentrations of the herbicide dichlorobenil and its persistent metabolite 2,6-dichlorobenzamide by *Aminobacter* spp. isolated from dichlorobenil-treated soils. *Appl. Environ. Microbiol.* 73:399–406. <http://dx.doi.org/10.1128/AEM.01498-06>.
17. Sørensen SR, Rasmussen J, Jacobsen CS, Jacobsen OS, Juhler RK, Aamand J. 2005. Elucidating the key member of a linuron-mineralizing bacterial community by PCR and reverse transcription-PCR denaturing gradient gel electrophoresis 16S rRNA gene fingerprinting and cultivation. *Appl. Environ. Microbiol.* 71:4144–4148. <http://dx.doi.org/10.1128/AEM.71.7.4144-4148.2005>.
18. Schmidt SK, Alexander M. 1985. Effects of dissolved organic carbon and second substrates on the biodegradation of organic compounds at low concentrations. *Appl. Environ. Microbiol.* 49:822–827.
19. Kovárová-Kovar K, Egli T. 1998. Growth kinetics of suspended microbial cells: from single-substrate-controlled growth to mixed-substrate kinetics. *Microbiol. Mol. Biol. Rev.* 62:646–666.
20. Lendenmann U, Snozzi M, Egli T. 1996. Kinetics of the simultaneous utilization of sugar mixtures by *Escherichia coli* in continuous culture. *Appl. Environ. Microbiol.* 62:1493–1499.
21. Aa K, Olsen RA. 1996. The use of various substrates and substrate concentrations by a *Hyphomicrobium* sp. isolated from soil: effect on growth rate and growth yield. *Microb. Ecol.* 31:67–76.
22. Egli T. 2010. How to live at very low substrate concentration. *Water Res.* 44:4826–4837. <http://dx.doi.org/10.1016/j.watres.2010.07.023>.
23. Sørensen SR, Aamand J. 2003. Rapid mineralisation of the herbicide isoproturon in soil from a previously treated Danish agricultural field. *Pest Manag. Sci.* 59:1118–1124. <http://dx.doi.org/10.1002/ps.739>.
24. Vital M, Fuchsli HP, Hammes F, Egli T. 2007. Growth of *Vibrio cholerae* O1 Ogawa Eltor in freshwater. *Microbiology* 153:1993–2001. <http://dx.doi.org/10.1099/mic.0.2006/005173-0>.
25. Vital M, Hammes F, Egli T. 2012. Competition of *Escherichia coli* O157 with a drinking water bacterial community at low nutrient concentrations. *Water Res.* 46:6279–6290. <http://dx.doi.org/10.1016/j.watres.2012.08.043>.
26. Hammes F, Berney M, Wang Y, Vital M, Köster O, Egli T. 2008. Flow-cytometric total bacterial cell counts as a descriptive microbiological parameter for drinking water treatment processes. *Water Res.* 42:269–277. <http://dx.doi.org/10.1016/j.watres.2007.07.009>.
27. Helbling DE, Hollender J, Kohler HPE, Singer H, Fenner K. 2010. High-throughput identification of microbial transformation products of organic micropollutants. *Environ. Sci. Technol.* 44:6621–6627. <http://dx.doi.org/10.1021/es100970m>.
28. Helbling DE, Hollender J, Kohler HPE, Fenner K. 2010. Structure-based interpretation of biotransformation pathways of amide-containing compounds in sludge-seeded bioreactors. *Environ. Sci. Technol.* 44:6628–6635. <http://dx.doi.org/10.1021/es101035b>.
29. Monod J. 1949. The growth of bacterial cultures. *Annu. Rev. Microbiol.* 3:371–394. <http://dx.doi.org/10.1146/annurev.mi.03.100149.002103>.
30. McCarty PL. 1965. Thermodynamics of biological synthesis and growth. *Air Water Pollut.* 9:621–639.
31. McCarty PL. 2007. Thermodynamic electron equivalents model for bacterial yield prediction: modifications and comparative evaluations. *Biotechnol. Bioeng.* 97:377–388. <http://dx.doi.org/10.1002/bit.21250>.
32. Rittmann BE, McCarty PL. 2001. Environmental biotechnology: principles and applications. McGraw-Hill, New York, NY.
33. VanBriesen JM. 2001. Thermodynamic yield predictions for biodegradation through oxygenase activation reactions. *Biodegradation* 12:265–281. <http://dx.doi.org/10.1023/A:1013179315518>.
34. R Development Core Team. 2013. R: a language and environment for statistical computing. R Foundation for Statistical Computing, Vienna, Austria.
35. Soetaert K, Petzoldt T. 2010. Inverse modelling, sensitivity and Monte Carlo analysis in R using package FME. *J. Stat. Softw.* 33:1–28.
36. Haario H, Laine M, Mira A, Saksman E. 2006. DRAM: efficient adaptive MCMC. *Stat. Comput.* 16:339–354. <http://dx.doi.org/10.1007/s11222-006-9438-0>.
37. Christensen DR, McCarty PL. 1975. Multiprocess biological treatment model. *J. Water Pollut. Control Fed.* 47:2652–2664.
38. Lawrence AW, McCarty PL. 1970. Unified basis for biological treatment design and operation. *J. Sanit. Eng. Div.* 96:757–778.
39. McCarty PL. 1975. Stoichiometry of biological reactions. *Prog. Water Technol.* 7:157–172.
40. Sørensen SR, Simonsen A, Aamand J. 2009. Constitutive mineralization of low concentrations of the herbicide linuron by a *Variovorax* sp. strain. *FEMS Microbiol. Lett.* 292:291–296. <http://dx.doi.org/10.1111/j.1574-6968.2009.01501.x>.
41. Robinson JA, Tiedje JM. 1983. Nonlinear estimation of monod growth kinetic parameters from a single substrate depletion curve. *Appl. Environ. Microbiol.* 45:1453–1458.
42. Cappuyens AM, Bernaerts K, Smets IY, Ona O, Prinsen E, Vanderleyden J, Van Impe JF. 2007. Optimal fed batch experiment design for estimation of monod kinetics of *Azospirillum brasilense*: from theory to practice. *Biotechnol. Prog.* 23:1074–1081.
43. Liu C, Zachara JM. 2001. Uncertainties of Monod kinetic parameters nonlinearly estimated from batch experiments. *Environ. Sci. Technol.* 35:133–141. <http://dx.doi.org/10.1021/es001261b>.
44. Lendenmann U, Snozzi M, Egli T. 2000. Growth kinetics of *Escherichia coli* with galactose and several other sugars in carbon-limited chemostat culture. *Can. J. Microbiol.* 46:72–80. <http://dx.doi.org/10.1139/cjm-46-1-72>.
45. Schaechter M, Maaloe O, Kjeldgaard NO. 1958. Dependency on medium and temperature of cell size and chemical composition during balanced growth of *Salmonella typhimurium*. *J. Gen. Microbiol.* 19:592–606. <http://dx.doi.org/10.1099/00221287-19-3-592>.
46. U.S. Environmental Protection Agency. 2012. Estimation Programs Interface (EPI) suite for Microsoft Windows, v4.11. United States Environmental Protection Agency, Washington, DC. <http://www.epa.gov/oppt/exposure/pubs/episuite.htm>.
47. Mavrouniotis ML. 1990. Group contributions for estimating standard Gibbs energies of formation of biochemical compounds in aqueous solution. *Biotechnol. Bioeng.* 36:1070–1082. <http://dx.doi.org/10.1002/bit.260361013>.
48. Tang A, Wang L, Zhou R. 2010. Gibbs energies of formation of chlorinated benzoic acids and benzoates and application to their reductive dechlorination. *Theochem* 960:31–39. <http://dx.doi.org/10.1016/j.theochem.2010.08.021>.